

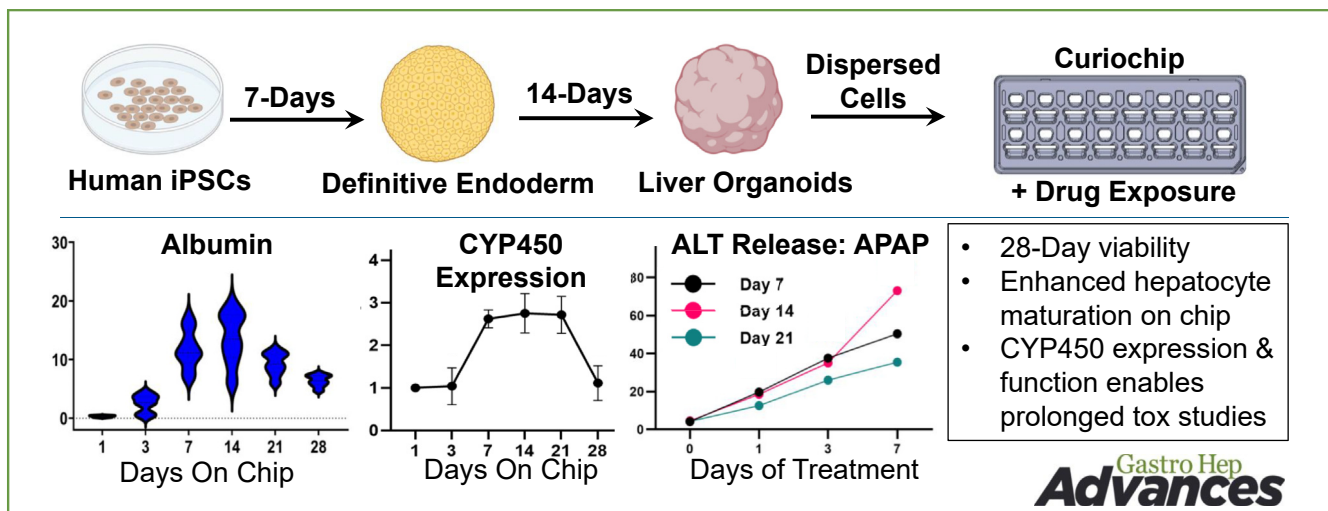
## ORIGINAL RESEARCH—BASIC

## A High-Throughput Microphysiological Liver Chip System to Model Drug-Induced Liver Injury Using Human Liver Organoids



Sophia R. Meyer,<sup>1,\*</sup> Charles J. Zhang,<sup>1,\*</sup> Max A. Garcia,<sup>2</sup> Megan C. Procario,<sup>2</sup> Sanghee Yoo,<sup>3</sup> Amber L. Jolly,<sup>3</sup> Sumin Kim,<sup>3</sup> Jiho Kim,<sup>3</sup> Kyusuk Baek,<sup>3</sup> Roland D. Kersten,<sup>1</sup> Robert J. Fontana,<sup>2</sup> and Jonathan Z. Sexton<sup>1,2</sup>

<sup>1</sup>Department of Medicinal Chemistry, College of Pharmacy, University of Michigan, Ann Arbor, Michigan; <sup>2</sup>Department of Internal Medicine, Gastroenterology and Hepatology, Michigan Medicine at the University of Michigan, Ann Arbor, Michigan; and <sup>3</sup>Qureator Inc, San Diego, California



**BACKGROUND AND AIMS:** Drug-induced liver injury (DILI) is a major failure mode in pharmaceutical development. This study aims to address the limitations of existing preclinical models by assessing a high-throughput, microfluidic liver-on-a-chip system, termed “Curio Barrier Liver Chips,” and its capacity to recapitulate the effects of chronic hepatotoxic drug treatment through metabolic and phenotypic characterization. **METHODS:** Curio Barrier liver chips (Curiochips), fabricated in an 8 × 2 well configuration, were utilized to establish three dimensional liver organoid cultures. Human-induced pluripotent stem cells were differentiated into human liver organoids, and their viability, liver-specific functions, and pharmacological responses were assessed over 28 days. **RESULTS:** The Curiochips successfully maintained liver physiology and function, showing strong albumin secretion and cytochrome (CYP) P450 activities for 28 days. Unlike traditional models requiring millimolar drug concentrations to detect hepatotoxicity, this platform showed increased sensitivity for acetaminophen and fialuridine at micromolar concentrations. *In situ* differentiation of foregut spheroids to liver organoids was also achieved, further simplifying the establishment of liver chips. Furthermore, the chips demonstrated viability, function, and DILI responsiveness for 28 days, making this an improved model for studying idiosyncratic DILI with prolonged drug exposure and

high-throughput capabilities compared to other available systems or primary human hepatocytes. **CONCLUSION:** The Curiochips offer an advanced, miniaturized *in vitro* model for early-stage drug development and a sensitive, responsive, and cost-effective means to detect direct hepatotoxicity. Induced pluripotent stem cell liver organoids, in conjunction with the Curiochip, deliver a high-throughput platform with robust functionality and pharmacological responsiveness that make it a promising tool for improving the prediction and understanding of DILI risk prediction, especially with prolonged drug exposure. The model also opens new avenues for research in other chronic liver diseases.

\*Co-first authors.

**Abbreviations used in this paper:** ALT, alanine transaminase; APAP, acetaminophen; DE, definitive endoderm; DILI, drug-induced liver injury; DRV, darunavir; FDA, US Food and Drug Administration; FIAU, fialuridine; HLO, human liver organoid; iPSC, induced pluripotent stem cell; LC, liquid chromatography; MPS, microphysiological system; MS, mass spectrometer; SBS, Society for Biomolecular Screening.

Most current article

Copyright © 2024 The Authors. Published by Elsevier Inc. on behalf of the AGA Institute. This is an open access article under the CC BY-NC-ND license (<http://creativecommons.org/licenses/by-nc-nd/4.0/>).

2772-5723

<https://doi.org/10.1016/j.gastha.2024.08.004>

**Keywords:** Drug-Induced Liver Injury; Hepatotoxicity; Microfluidic Liver Chips; Microphysiologic Liver System; High-Throughput Screening; iPSC-Derived Human Liver organoids; DILI Model; Curiochips

## Introduction

Drug-induced liver injury (DILI) represents a significant challenge in both medical practice and drug development.<sup>1,2</sup> The liver, being the principal organ for drug metabolism and detoxification, is highly susceptible to damage caused by exogenous compounds. Hepatotoxicity in drug candidates is often not predicted in standard preclinical models nor observed in early clinical studies. The late-stage detection of DILI in clinical studies and post-US Food and Drug Administration (FDA) approval is a significant failure point in drug development and a leading cause for FDA regulatory actions.<sup>3,4</sup> Indeed, an estimated 22% of clinical trial failures and 32% of market withdrawals of novel molecular entities are due to unanticipated hepatotoxicity.<sup>5,6</sup> As there are currently over 2500 prescription medications and >80,000 herbal and dietary supplements available for use in the United States, the potential for additive or synergistic liver toxicity is high, and the current available *in vivo* and *in vitro* DILI models have low and inadequate predictive capability.<sup>7,8</sup> Improving preclinical models to enhance stability over time and recapitulate liver pathophysiology will not only reduce drug attrition rates in clinical trials and postmarketing, but it will also enable the study of the more complex DILI mechanism, termed “idiosyncratic,” that occurs in small subsets of patients often weeks after the agent is discontinued. Recent advancements in multicompartiment *in vitro* microphysiologic liver-on-a-chip systems that use pumps to achieve tangential media flow have allowed for higher fidelity preclinical prediction of hepatotoxicity compared to conventional two dimensional (2D) monolayer culture systems.<sup>8–11</sup> While many of these microfluidic models maintain cadaveric primary human hepatocytes or induced pluripotent stem cell (iPSC)-derived liver organoids for longer than traditional assays, there are still prominent differences in culture longevity, cost, throughput, and scalability across existing platforms.

The lack of viable long-term *in vitro* liver models poses a significant limitation in investigating direct and idiosyncratic DILI. Clinical evidence indicates that DILI often manifests weeks or even months into a treatment regimen or even weeks after the discontinuation of a drug.<sup>12,13</sup> Clinically, idiosyncratic DILI also exhibits a high degree of heterogeneity in its presentation and severity. In many cases, liver injury does not improve following the withdrawal of the offending drugs, and it may even continue to worsen. Our understanding of the genetic and environmental factors contributing to idiosyncratic DILI risk remains limited despite extensive *in vitro* and preclinical testing of all new molecular entities during their development.<sup>14,15</sup> These complex phenomena cannot be effectively modeled without

the availability of long-term hepatocyte culture models that maintain physiological relevance for extended periods after seeding or patterning with multiple liver and immune cell types. In addition, the demand for an effective long-term liver model extends beyond the study of idiosyncratic DILI with prolonged drug dosing. Other common chronic liver diseases such as metabolic-associated steatotic liver disease, fibrosis, and chronic viral hepatitis also highlight the unmet need for robust, long-term multicellular liver models to facilitate future natural history and mechanistic studies.

This study describes the development of a high-throughput and low-cost microphysiologic system (MPS) for evaluating drug-induced hepatotoxicity. Unlike existing liver MPS which use motorized pumps to maintain media flow, the Qureator Curiochip platform used in this study relies on passive osmotically driven media flow. Here, we demonstrate the functionality of iPSC-derived multicellular human liver organoids (HLOs) on the Qureator Curiochip platform through phenotypic and metabolic assessment of naïve hepatocytes in culture media, necrotic injury following acetaminophen (APAP) treatment, and mitochondrial toxicity following fialuridine (FIAU) treatment. Finally, we demonstrate the ability of this MPS to maintain cellular health and function for up to 28 days, which allows for experiments involving prolonged assay time points like those required to study idiosyncratic DILI.

## Methods

### Curiochip Preparation for 3D Patterning

A detailed protocol for Curiochip preparation for three dimensional (3D) patterning is described in Kim et al, 2023.<sup>16</sup> In brief, the 16-well Curio-Barrier Microphysiological System integrates seamlessly into a custom Society for Biomolecular Screening (SBS)-format plate adapter, accommodating automated high-content and high-throughput screening. Constructed using injection-molded polystyrene and bonded with a polycarbonate bottom via adhesive film, the chip features 3 distinct channels: a central channel lined with hydrogel for media and cell support, flanked by 2 side channels designed for sequential tissue structuring. This design enables the stable formation of cellular barriers and supports the seeding and differentiation of liver organoid cells in physiologically relevant configurations.

### Human Liver Organoid Differentiation and Chip Culture

HLOs were differentiated as previously described.<sup>9</sup> In brief, human iPSC line 72.3 obtained from Cincinnati Children’s Hospital Medical Center was differentiated into HLOs based on a previously described protocol.<sup>17</sup> iPSCs were seeded at high density on growth factor-reduced Matrigel (Corning, 354230)-coated 6-well plates (Thermo Fisher Scientific, 140675) to achieve 90% confluency after 24 hours of culture. iPSCs were treated with Activin A (R&D Biosystems, 338-AC) for 3 days and FGF4 (purified in-house) for 3 additional days to bud definitive endoderm (DE) spheroids.

DE spheroids were embedded in 75  $\mu\text{L}$  Matrigel (Corning, 354234) droplets in 6-well plates and treated with retinoic acid for 4 days followed by hepatocyte growth media (Hepatocyte Culture Medium BulletKit [Lonza, CC-3198] supplemented with 10 ng/mL hepatocyte growth factor [PeproTech, 100-39], 20 ng/mL oncostatin M [R&D Systems, 2950M050], and 0.1  $\mu\text{M}$  dexamethasone [Millipore Sigma, D4902]) for 16 days. Following culture, cells were removed from Matrigel embeddings by mechanical dislodging with 10 mL wash media (DMEM/F12 supplemented with 1X pen/strep). In 15 mL tubes, organoids in Matrigel were broken apart by repetitive pipetting and spun down at  $300 \times g$  for 3 minutes. Media and Matrigel were carefully aspirated before repeating washing with fresh 10 mL of wash media. This procedure was repeated until most Matrigel residue was visually removed following roughly 3–5 washes.

Free organoids were then dispersed by resuspension in 0.25% trypsin and were transferred to a 6-well plate for 37 °C incubation. After 10 minutes of incubation, cells were pipetted up and down and returned to the incubator for an additional 5 minutes. Trypsin activity was stopped by adding 1 mL fetal bovine serum, transferred to a fresh 15 mL tube, and spun down at  $500 \times g$  for 5 minutes. Trypsin with fetal bovine serum was then aspirated, and cells were resuspended in PBS and passed through a 100  $\mu\text{m}$  filter. Cells in phosphate buffered saline were then counted for downstream applications.

### Curiochip Patterning and Culture

Dispersed HLOs were resuspended in a hydrogel mixture of Rat Tail Collagen Type 1 (Corning, 354236) and Matrigel (Corning, 354230) at a density of 10,000 cells per 1.4  $\mu\text{L}$  and kept on ice. 1.4  $\mu\text{L}$  of this hydrogel cell suspension was pipetted into the middle channel of each Curiochip well and was incubated at 37 °C for 15 minutes to solidify. An additional volume of cell-free hydrogel mixture was loaded into the side 1 channel and the culture medium was patterned into the side 2 channel and incubated at 37 °C for 15 minutes to solidify. 100  $\mu\text{L}$  of complete hepatocyte growth media was added to the top reservoir, while 20  $\mu\text{L}$  was added to the bottom reservoir to create a volume gradient that would allow for gradual flow. Media was collected and changed 1 day after patterning, followed by every other day.

For assessing the differentiation of DE to HLOs, foregut spheroids from day 7 of the differentiation protocol were resuspended in the hydrogel mixture and loaded into the middle channel of the Curiochips instead of dispersed HLOs. Following solidification and hydrogel addition to the side 1 and 2 channels, the differentiation media were identical to standard HLO differentiation. 100  $\mu\text{L}$  of each media was added to both reservoirs (no flow) until the addition of hepatocyte growth media, where 100  $\mu\text{L}$  of media was added to the top reservoir and 20  $\mu\text{L}$  in the bottom reservoir to introduce flow.

### Human Serum Albumin and ALT Measurements

50  $\mu\text{L}$  of media from both reservoirs for each chip well was collected and pooled at respective time points. Albumin from chip media outflow was measured using enzyme-linked immunosorbent assay (ELISA) (R&D Systems, DY1455). 10  $\mu\text{L}$  of media was diluted 100-fold in PBS before incubation on an ELISA plate. A standard curve was created with albumin

concentrations ranging from 2.5 to 160 ng/mL. Each sample was assayed in triplicate, and results were scaled per  $10^6$  cells.

For measuring ALT, 30  $\mu\text{L}$  of media and PBS were dispensed into a 96-well assay plate. 300  $\mu\text{L}$  of room temperature ALT/GPT reagent (Thermo Fisher Scientific, TR71121) was then dispensed into all wells in the plate and incubated at 37 °C for 30 seconds before recording absorbance at 340 nm for 3 minutes. The activity of ALT was determined using the following equation:

$$\text{Abs} / \text{min} \times \text{Factor}$$

The Factor constant is predetermined for this assay as 1746, using the manufacturer's recommendation. The average absorbance from blanks was subtracted from all other samples. Plates were read with a BioTek Synergy H1 Microplate Reader.

### CYP450 Relative Gene Expression

RNA was purified with the Direct-zol RNA Miniprep (Zymo Research, R2052) and expression was measured using CFX96 Touch Deep Well Real-Time PCR System (BioRad) and iTaq Universal Probes One-Step Kit (BioRad, 1725141). Primers used were CYP1A1 (Thermo Fisher Scientific, Hs01054796\_g1), CYP2D6 (Hs04931916\_gH), CYP3A4 (Hs00604506\_m1), and housekeeping gene GAPDH (Thermo Fisher Scientific, Hs02786624\_g1). Fold change was calculated using the  $\Delta\Delta\text{Ct}$  method over day 1 HLOs on Curiochips.<sup>18</sup>

### CYP450-Mediated Substrate Metabolism

APAP, cyclophosphamide, and darunavir (DRV) were chosen as substrates for CYP 1, 2, and 3 families, respectively. The media in Curiochips was replaced with 100  $\mu\text{L}$  of media in each reservoir containing substrates at 10  $\mu\text{M}$ . After 1 hour and 2 hours of incubation, 50  $\mu\text{L}$  of media from each reservoir was pooled to achieve 100  $\mu\text{L}$  of total media for analysis. Reactions were stopped using 100  $\mu\text{L}$  of cold methanol and centrifuged for 5 minutes at 3000 revolutions per minute to collect the supernatant. Samples were analyzed by quantitative LC/MS/MS to detect the diminution in the drug parent mass using a Thermo ESI-Q-Exactive Orbitrap mass spectrometer coupled to a Thermo Vanquish ultra-HPLC system. Experimental variables include a Phenomenex Kinetex 2.6  $\mu\text{m}$  C18 reverse phase 100 Å  $150 \times 3$  mm liquid chromatography (LC) column, 2  $\mu\text{L}$  injection volume; LC gradient, solvent A, 5% acetonitrile and 0.1% formic acid; solvent B, 100% acetonitrile and 0.1% formic acid; 0 min, 0% B; 1 min, 0% B; 7 min, 80% B; flow rate 0.4 mL/min; mass spectrometer (MS), and positive ion mode was used.

### Image Acquisition

Confocal fluorescence images were acquired with a Yokogawa CQ1 or CellVoyager 8000 High-Content Screening System in a custom-fabricated SBS plate format Curiochip holder. Each holder accommodates 3 Curiochips, totaling 48 wells per imaging cycle. 3D images were acquired on the CQ1 using a 10X/0.4NA objective lens by obtaining 10 Z-planes across a 100  $\mu\text{m}$  range. Imaging on the CellVoyager 8000 system was performed using a 20X/1.0NA water immersion objective lens where 1  $\mu\text{m}$  Z-stacks were obtained across 150  $\mu\text{m}$  to produce maximum intensity projection images for analysis.

### Quantification and Statistical Analysis

Statistical analyses were performed using GraphPad Prism (version 9.5). Assays were performed across biological replicates with a minimum of 3 replicates. Paired conditions were analyzed using either repeated measure one-way ANOVA with Tukey's *post hoc* test or two-way ANOVA with Sidak or Dunnett's *post hoc* test, depending on the comparisons made. Unpaired data were analyzed using two-way ANOVA with Tukey's *post hoc* test or the Kruskal-Wallis test for nonparametric data. *P* values < .05 were considered statistically significant. The *n*-value refers to biologically independent replicates. All images quantified for biomarker intensities were analyzed using Cellprofiler (4.2.5)<sup>19</sup> per image field-of-view. Statistical parameters are denoted in the figures and figure legends.

## Results

### Design and Engineering of a High-Throughput Microfluidic Liver Chip

Curiochips, developed by Qureator Inc, were engineered with 16 wells in an 8 × 2 configuration, allowing for the establishment of 3D or 2D liver organoid cultures embedded in a mixture of collagen type 1 and Matrigel. Wells were designed to allow for patterning in 3 channels (side 1, side 2, and the middle channel), allowing for varying hydrogel and cell types without membrane separation and including 2 media reservoirs. Curiochips are SBS plate-compatible to facilitate high-throughput screening screening using a liquid handler and high-content imaging-based characterization. HLOs were dispensed in the middle channel of the Curiochip, and an acellular hydrogel was patterned into the side 1 channel. The culture medium was dispensed into the side 2 channel (Figure 1).

### Twenty-Eight-Day HLO Function and Metabolism in High-Throughput Curiochips

For these studies, human iPSC line 72.3 cells obtained from Cincinnati Children's Hospital Medical Center were differentiated into HLOs based on a previously described

protocol.<sup>9,17</sup> Each well contained 2 media ports and for our purposes of developing HLO liver chips, these ports were used with media gradients to achieve a steady hydrostatic media flow. With an emphasis on designing a high-throughput, SBS-plate-compatible format, media collection and maintenance were achieved in Curiochips by standard multichannel pipettors/automated liquid handlers.

Dispersed HLO cells dispensed and cultured in Curiochips with hydrostatic media flow remained visually consistent in morphology and cell density across 7 days of on-chip culture (Figure A1). HLOs were cultured on Curiochips for 28 days for further assessment of hepatic function. Similarly to our previous reports of HLO albumin expression on microfluidic chips, periodic assaying of output media demonstrated consistent albumin production through day 7 with reduced but persistent secretion measured at 28 days (Figure 2A).<sup>9</sup> Evidence of stimulated HLO maturation on Curiochips was observed, and fluctuations in CYP450 expression levels over 28 days in culture ( $F(5, 36) = 14.04$ ;  $P < .0001$ ) are also observed (Figure 2B). Notably, the HLO expression of CYP450s trended upward until the peak expression was reached by days 7–21 of the Curiochip culture. HLOs matured on Curiochips for 7 days were assessed for their metabolic function by measuring the turnover of toxic doses of APAP, metabolized by conjugation and CYP 2E1 and DRV, metabolized exclusively by CYP 3A4. When comparing HLOs cultured in static media on standard tissue culture plates to those cultured on Curiochips, there is a notable difference in the metabolism of DRV and APAP. Specifically, HLOs on Curiochips demonstrate a higher degree of DRV metabolism and a comparable extent of APAP metabolism than those in static culture conditions (Figure 2C). This finding suggests that hepatocyte maturation on Curiochips enables enhanced CYP3A4 functionality but no significant difference in parent compound conjugation or CYP2E1 activity. CYP450 expression and activity were comparable to our previous report of HLOs matured on a microfluidic device, and the time-dependent maturation and functionality of HLOs on Curiochips, as well as other microfluidic devices, suggest careful consideration

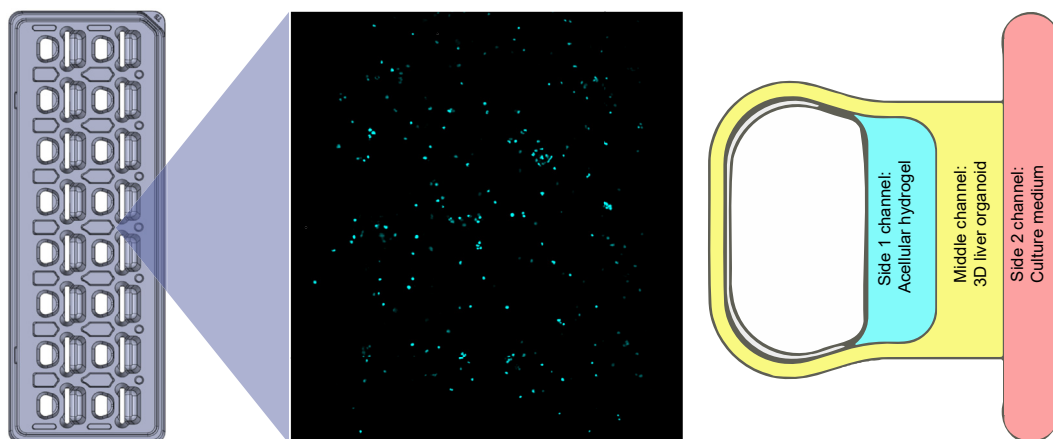


**Figure 1.** Diagram of a 16-well HLO Curiochip with a fluorescent image of a single well and detailed configuration.



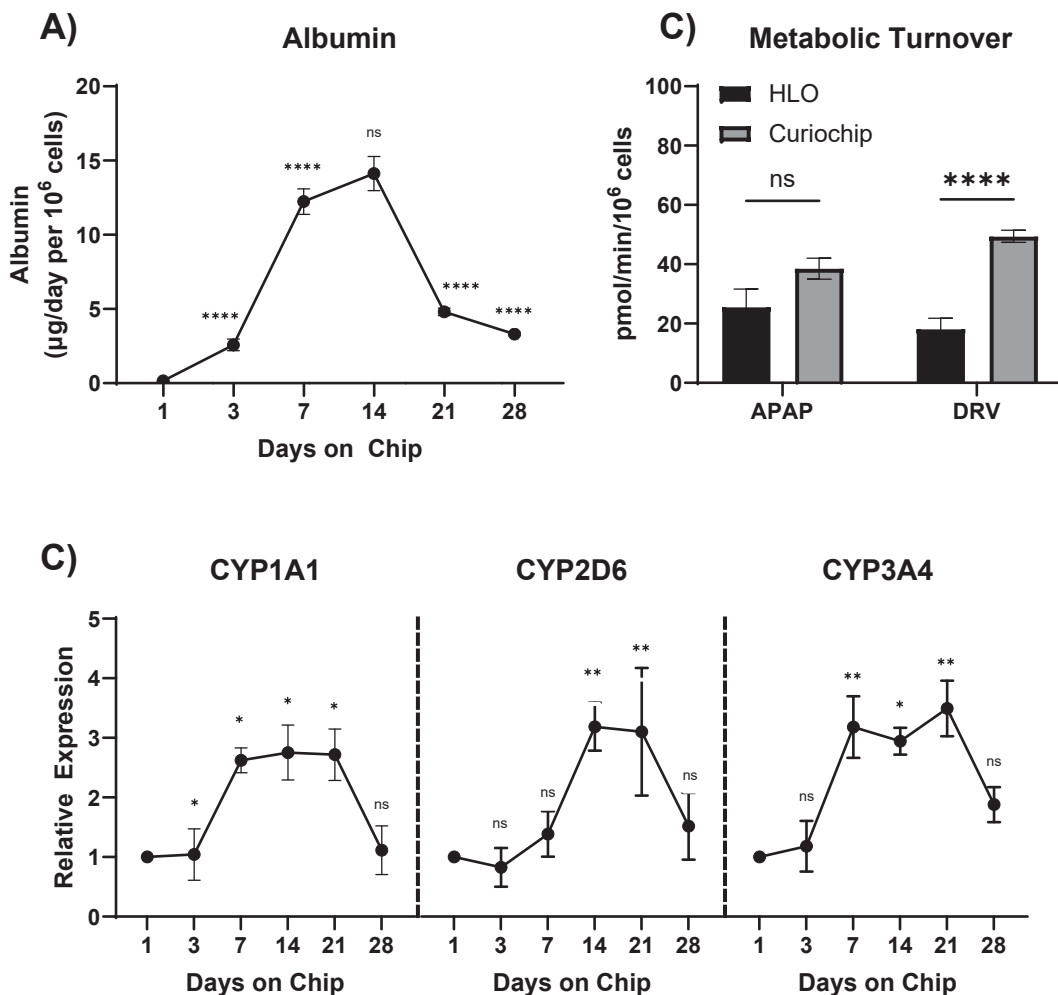


**Figure 2.** Twenty-eight-day Curiochip HLO viability. (A) HLOs were plated on Curiochips, and output media was periodically assessed for albumin secretion ( $n = 16$ ). (B) CYP450 gene expression was quantified from parallel time points after cell lysis ( $n = 3$ ). Data were compared to day 14 Curiochips. (C) Day 7 Curiochip cultures were assessed for metabolic function by quantifying molecular turnover of acetaminophen (APAP) and darunavir (DRV) exclusively metabolized by CYP450s using LC/MS/MS;  $n = 3$  and 16 for HLO and Curiochips, respectively. Data are expressed as mean  $\pm$  standard error of the mean. \* $P < .05$ ; \*\* $P < .01$ ; \*\*\* $P < .001$ ; \*\*\*\* $P < .0001$ ; n.s., not significant.

when developing assay time points and normalization methods.<sup>9</sup> Additionally, compound dosing within Curiochips featuring hydrogel patterning reveals no intrinsic compound absorption by the device itself (Figure A2). This indicates that when conducting metabolic studies on Curiochips, there is no need to adjust data based on the anticipated compound absorption into plastic coatings, as is necessary with other liver microfluidic devices.

### Twenty-Eight-Day Microfluidic Liver Chips as a Long-Term Model of DILI

After identifying the time dependence of HLO function on Curiochips, we investigated the kinetics of function and responsiveness of this platform in drug-mediated injury. To model clinically relevant DILI mediated by compounds with distinct mechanisms and phenotypes, we exposed Curiochips at different days of culture and maturation to

clinically characterized small molecule drugs to assess the effects of kinetic hepatocellular function on readouts of hepatocellular injury. HLOs were matured on Curiochips for 7, 14, or 21 days of culture before being treated with 7-day exposure to bona fide DILI-causing agents (Figure 3A). Specifically, we chose APAP as one of our controls due to its status as the leading cause of acute liver failure in the United States, characterized by hepatocellular necrosis.<sup>20</sup> Additionally, FIAU was selected as another control based on its history as a clinical candidate that caused multiple patient deaths in clinical trials due to unpredicted hepatotoxicity. Our group and others have previously modeled FIAU-induced hepatotoxicity in HLOs and other 3-dimensional models of human hepatocytes, demonstrating lipid accumulation and elevated ALT levels as hallmarks of injury.<sup>9,21</sup> We assessed hepatocellular injury of day 7, 14, and 21 Curiochips by quantifying albumin concentrations and alanine transaminase (ALT) activity after APAP

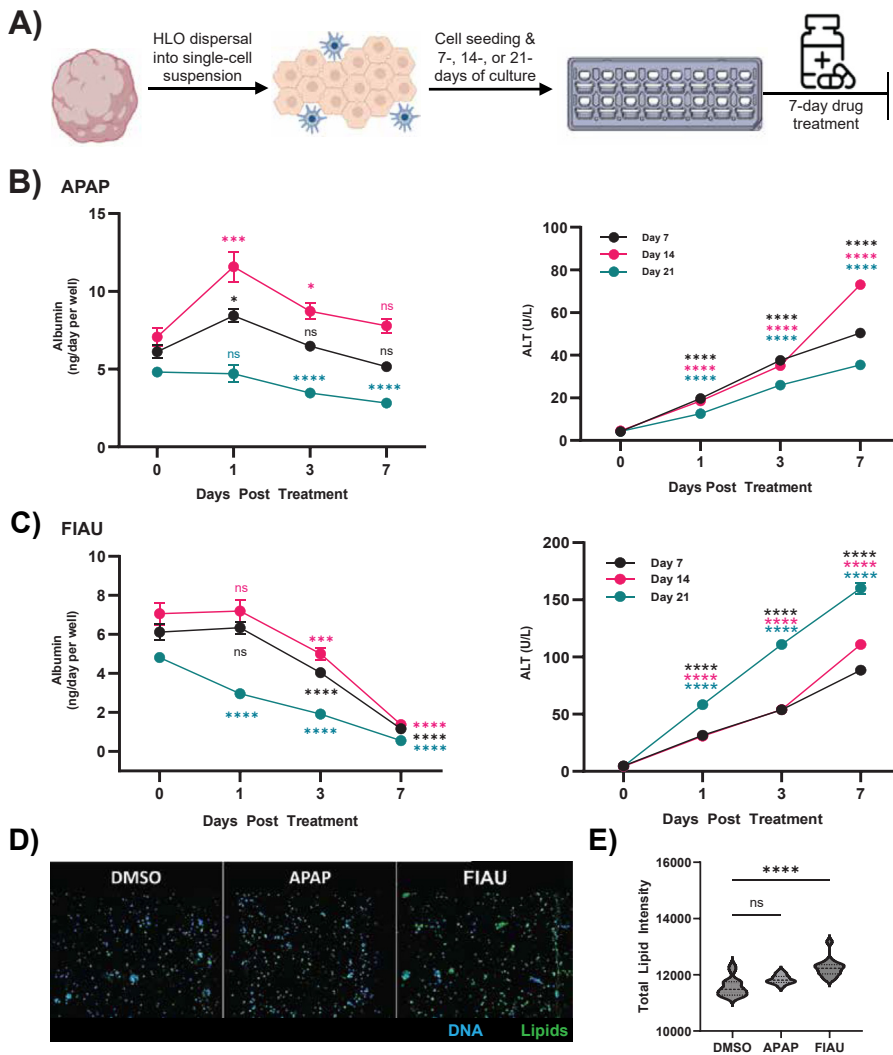


**Figure 3.** Functional and phenotypic assessment of Curiochips as a long-term DILI model. (A) Schematic drawing of chronic DILI assay using HLOs on Curiochips. Curiochips were treated for 7 days with either (B) APAP or (C) FIAU and assessed for kinetic hepatocyte function and injury through biochemical analysis of albumin secretion and ALT activity. Multiple comparisons were made between sequential drug treatment time points. (D) Fluorescent images of vehicle control and drug-treated Curiochips stained for DNA and neutral lipid droplets were (E) quantified for total lipid intensity. Data are expressed as mean  $\pm$  SEM of  $n = 16$  Curiochips per treatment group. \* $P < .05$ ; \*\* $P < .01$ ; \*\*\* $P < .001$ ; \*\*\*\* $P < .0001$ ; n.s., not significant.

(Figure 3B) and FIAU incubation (Figure 3C). During the 7-day APAP treatment, both treatment time ( $F(2,212, 99.53) = 55.44$ ;  $P < .0001$ ) and days cultured on the Curiochip ( $F(6, 135) = 5.569$ ;  $P < .0001$ ) contributed most of the variation in albumin concentrations. Though significantly decreased from baseline, Curiochips cultured for 21 days before drug treatment did not show a significantly steady decrease in albumin concentration throughout 2-day time points during APAP treatment. In contrast, Curiochips that matured for 7 and 14 days showed a more significant decrease in albumin concentration throughout 7 days of treatment. These observed changes in albumin response strongly correlate with quantifications of ALT activity, which exhibited a rapid escalation following one day of drug exposure. The lowest level of ALT activity was demonstrated from day 21 Curiochips, which also had the lowest surveyed albumin concentrations. FIAU treatment induced a similar trend in decreasing albumin concentrations observed under APAP treatment. Particularly noteworthy, however, is the heightened ALT activity upon FIAU exposure in the 21-day Curiochip compared to the 14- and 7-day

counterparts. In contrast, the response to APAP exposure was least pronounced in the 21-day Curiochip model. This discrepancy suggests a less prominent CYP2 family-mediated metabolism of APAP to N-acetyl-p-benzoquinone imine in the 21-day Curiochips. Given that the 21-day Curiochips subjected to drug treatment for 7 days underwent a total culture period of 28 days, this observation aligns with the diminished 28-day CYP450 expression data discussed above.

To assess the phenotypic injury induced by both control drugs, 14-day Curiochips were fixed at the end of the 7-day drug exposure and stained for DNA and lipid droplets (Figure 3D). FIAU treatment induced an accumulation of lipid droplets compared to the dimethyl sulfoxide control (Figure 3E), which is characteristic of FIAU-induced steatohepatitis histopathology.<sup>22</sup> Though APAP treatment did not alter lipid accumulation or overt cell death (Figure A3), the significant increase in ALT response may suggest a compensatory mechanism either preventing hepatocyte death or inciting a consistent cell proliferation rate.

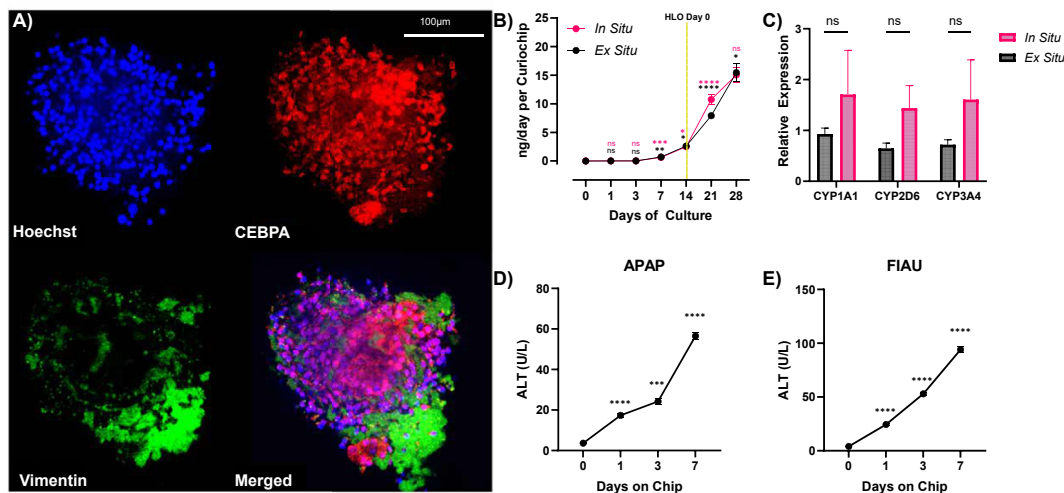


**Figure 4.** *In situ* differentiation of HLOs on Curiochips. (A) Confocal fluorescence imaging of HLOs differentiated directly on Curiochips with cell-specific staining of hepatocytes (CEBPA) and hepatic stellate cells (vimentin). (B) Kinetic albumin secretion from *in situ* and *ex situ* differentiation of HLOs ( $n = 16$ ). Multiple comparisons were made between sequential days of culture. The yellow dotted line represents the date of complete HLO differentiation (corresponds to day 0 in Figure 2). (C) CYP450 gene expression ( $n = 3$ ) from *in situ* differentiated Curiochips compared to *ex situ* differentiation, both at day 21 of differentiation. DILI model evaluation of *in situ* Curiochips was quantified by ALT activity after (D) APAP and (E) FIAU treatments, over ( $n = 16$  for each condition). Data are expressed as mean  $\pm$  SEM; \* $P < .05$ ; \*\* $P < .01$ ; \*\*\* $P < .001$ ; \*\*\*\* $P < .0001$ ; n.s., not significant.

### *In Situ* Differentiation of Foregut Spheroids to HLOs on Curiochips

As the Curiochips allow for dispensing HLO cells embedded in hydrogel, we sought to test the capability of an *in situ* differentiation of DE spheroids to HLOs within the device. DE spheroids were prepared per our 7-day protocol before embedding them into hydrogel on Curiochips to complete the 14-day 3D HLO differentiation. Day 0 HLOs were then kept in 3D culture on Curiochips for an additional 14 days (28 days total culture on Curiochips) or treated with drugs for an additional 7 days (21 days total culture on Curiochips). *In situ* differentiated HLOs, as anticipated, showed positivity for hepatocytes (CEBPA) and mesenchymal stellate cells (vimentin) (Figure 4A). High-content imaging demonstrated that hepatocyte and stellate staining is regional, showing selective liver cell differentiation, particularly with the dissipation of vimentin staining in the HLO core. This suggests that *in situ* differentiation on Curiochips may result in regional heterogeneity, unlike the conventional, homogeneous dispersal method described above.

Kinetic assessment of hepatocyte maturity from *in situ* differentiation on Curiochips vs *ex situ* differentiation off-chip did not suggest reduced model function by any metric. The differentiation method did not significantly impact albumin secretion ( $F(1, 26) = 1.157$ ;  $P = .2921$ ), with both *in situ* and conventional *ex situ* differentiation methods displaying a substantial increase in albumin secretion as early as 7 days postcompletion of the HLO differentiation protocol (Figure 4B). *In situ* and *ex situ* 3D HLOs accelerate in albumin secretion at 7 days of HLO

maturation (14 days of total Curiochip culture), similar to the conventional single-cell HLO dispersal method discussed in preceding sections (direct comparisons not shown). Additionally, *in situ* differentiation did not significantly alter the CYP450 expression ( $F(1, 12) = 3.734$ ;  $P = .0773$ ) with CYP1A1, CYP2D6, and CYP3A4 expression staying relatively consistent compared to *ex situ* differentiation (Figure 4C). Lastly, *in situ* differentiated Curiochips show a consistent increase in ALT release to APAP and FIAU across 7 days of drug treatment (Figure 4E), as was previously seen with conventional *ex situ* differentiation described above. These observations suggest that reducing time, protocol steps, and labor involved with standard differentiation off-chip by utilizing *in situ* differentiation does not reduce model performance for drug-induced hepatotoxicity assessment.

## Discussion

This study explored the capacity of HLOs cultured on the Curiochip, a high-throughput microphysiological platform, to emulate physiological liver functions and faithfully reproduce DILI along with pertinent pathophysiological features. It has been previously identified that HLO culture on MPS enhances the sensitivity of drug toxicity testing and recapitulates agent-specific liver injury phenotypes. Still, the cost, scalability, and incompatibility with compound dosing are inherent aspects of MPS that have limited their wide-scale adoption. The results from this study suggest that newer generation, high-throughput, MPS such as the Curiochip can mitigate the limitations of previous MPS generations.

The inherent characteristics of existing microfluidic systems include high costs, low throughput, and complex drug pharmacokinetics. These factors significantly restrict batch sizes, limit experimental power by restricting replicates, hinder experimental conditions that can be investigated, and impede kinetic assessments. Another issue with many microfluidic devices is the choice of materials, often relying on polydimethylsiloxane or other highly drug-adsorbent materials.<sup>23</sup> These materials can lead to artifactual observations in drug effects and kinetics, potentially compromising the reliability of experimental results. To address these multiple challenges, we utilized scalable iPSC-derived HLOs and incorporated them into the Curiochip, an engineered high-throughput microfluidic platform, with a primary focus on enhancing consistency across replicates and minimizing inherent drug interactions to ensure robustness, particularly when applied to large-scale compound testing. Additionally, this model encompasses multiple liver cell types, including parenchymal hepatocytes and nonparenchymal hepatic stellate cells that may enhance the predictive power in DILI risk assessment. This system has been designed to integrate with standard laboratory automation, facilitating various analytical techniques such as biochemical bioassays, and high-content confocal immunofluorescence imaging. Despite its compact size, this liver-on-a-chip architecture retains essential features, including the ability to control media flow with liver organoids embedded into extracellular matrix scaffolds.

We envision that this system can significantly enhance the rigor and reproducibility in preclinical DILI risk assessment, thereby reducing attrition in drug development due to DILI and enhancing patient safety in clinical studies and post-FDA approval. Another major improvement enabled by higher throughput methods is the screening of multiple patient-derived organoids to predict the risk of liver injury across patients with diverse genetics who have experienced DILI. Furthermore, the Curiochip sandwich architecture makes it well-suited for testing compounds with longer drug exposure periods or therapeutic regimes that include a series of treatments, which can be invaluable in detecting single-agent or polypharmacology DILI in preclinical drug development to assist in triage of molecular entities in lead optimization.

Although the level of complexity associated with multicellular 3D cultures and dynamic fluid flow has shown to be a key factor in improved models, these features have not been compatible with high-throughput platforms and automated liquid handlers. However, our efforts effectively miniaturize the complex organ-on-chip systems to achieve higher throughput without sacrificing environmental conditions that deliver high physiological performance. This enables HLO Curiochips to be a cost-effective and rapid means for early-stage drug discovery testing for efficacy and safety testing. The scalability to 96 wells per plate also allows for complex studies, including those with large dose ranges and multidrug combinations compared to earlier-generation microfluidic liver chip systems.

Our findings suggest that miniaturized liver chips can support the long-term maintenance of iPSC-derived liver cells. Currently, models for idiosyncratic DILI with prolonged drug exposure and other chronic liver diseases are limited in terms of the treatment time frame. HLO Curiochips showed the ability to maintain viable liver cells for up to 28 days and demonstrated their utility in low-dose, long-term studies or liver recovery/regeneration research. This long-term model may also be useful in studying other chronic liver diseases, such as viral hepatitis. Future studies with HLO Curiochips will utilize improved scalability, extended assay time points, and pharmacokinetic improvements to develop and optimize models of idiosyncratic DILI using patient-derived HLOs, chronic drug exposure, and complex assay conditions.

## Supplementary Materials

Material associated with this article can be found in the online version at <https://doi.org/10.1016/j.gastha.2024.08.004>.

## References

1. Fontana RJ, Watkins PB, Bonkovsky HL, et al. Drug-Induced Liver Injury Network (DILIN) prospective study: rationale, design and conduct. *Drug Saf* 2009; 32(1):55–68.
2. Fontana RJ, Seeff LB, Andrade RJ, et al. Standardization of nomenclature and causality assessment in drug-induced liver injury: summary of a clinical research workshop. *Hepatology* 2010;52(2):730–742.
3. Stevens JL, Baker TK. The future of drug safety testing: expanding the view and narrowing the focus. *Drug Discov Today* 2009;14(3–4):162–167.
4. Wysowski DK, Swartz L. Adverse drug event surveillance and drug withdrawals in the United States, 1969–2002: the importance of reporting suspected reactions. *Arch Intern Med* 2005;165(12):1363–1369.
5. Bakke OM, Manocchia M, de Abajo F, et al. Drug safety discontinuations in the United Kingdom, the United States, and Spain from 1974 through 1993: a regulatory perspective. *Clin Pharmacol Ther* 1995;58(1):108–117.
6. Watkins PB. Drug safety sciences and the bottleneck in drug development. *Clin Pharmacol Ther* 2011; 89(6):788–790.
7. National Center for Health Statistics (US). *Health, United States, 2019*. Hyattsville, MD: National Center for Health Statistics (US), 2021.
8. Jang KJ, Otieno MA, Ronxhi J, et al. Reproducing human and cross-species drug toxicities using a liver-chip. *Sci Transl Med* 2019;11(517):eaax5516.
9. Zhang CJ, Meyer SR, O'Meara MJ, et al. A human liver organoid screening platform for DILI risk prediction. *J Hepatol* 2023;78(5):998–1006.
10. Ewart L, Apostolou A, Briggs SA, et al. Qualifying a human liver-chip for predictive toxicology: performance assessment and economic implications. *bioRxiv*



- [Internet]. biorxiv.org. 2021. <https://www.biorxiv.org/content/10.1101/2021.12.14.472674.abstract>. Accessed March 5, 2024.
11. Ewart L, Apostolou A, Briggs SA, et al. Performance assessment and economic analysis of a human liver-chip for predictive toxicology. *Commun Med (Lond)* 2022; 2(1):154.
  12. Reuben A, Tillman H, Fontana RJ, et al. Outcomes in adults with acute liver failure between 1998 and 2013: an observational cohort study. *Ann Intern Med* 2016; 164(11):724–732.
  13. Reuben A, Koch DG, Lee WM, Acute Liver Failure Study Group. Drug-induced acute liver failure: results of a U.S. multicenter, prospective study. *Hepatology* 2010; 52(6):2065–2076.
  14. Chalasani N, Bonkovsky HL, Fontana R, et al. Features and outcomes of 899 patients with drug-induced liver injury: the DILIN prospective study. *Gastroenterology* 2015;148(7):1340–1352.e7.
  15. Fontana RJ, Hayashi PH, Gu J, et al. Idiosyncratic drug-induced liver injury is associated with substantial morbidity and mortality within 6 months from onset. *Gastroenterology* 2014;147(1):96–108.e4.
  16. Kim J, Song Y, Jolly A, et al. Design and validation of a high-throughput in vitro model of the outer Blood-Retinal Barrier (oBRB) using the Curiochips Microphysiological System [Internet]. bioRxiv. 2023. <https://www.biorxiv.org/content/10.1101/2023.12.01.569537v1>. Accessed April 15, 2024.
  17. Thompson WL, Takebe T. Generation of multi-cellular human liver organoids from pluripotent stem cells. *Methods Cell Biol* 2020;159:47–68.
  18. Livak KJ, Schmittgen TD. Analysis of relative gene expression data using real-time quantitative PCR and the 2(-Delta Delta C(T)) Method. *Methods* 2001;25(4): 402–408.
  19. Stirling DR, Swain-Bowden MJ, Lucas AM, et al. Cell-Profiler 4: improvements in speed, utility and usability. *BMC Bioinformatics* 2021;22(1):433.
  20. Jaeschke H, Ramachandran A, Chao X, et al. Emerging and established modes of cell death during acetaminophen-induced liver injury. *Arch Toxicol* 2019; 93(12):3491–3502.
  21. Hendriks DFG, Hurrell T, Riede J, et al. Mechanisms of chronic fialuridine hepatotoxicity as revealed in primary human hepatocyte spheroids. *Toxicol Sci* 2019; 171(2):385–395.
  22. McKenzie R, Fried MW, Sallie R, et al. Hepatic failure and lactic acidosis due to fialuridine (FIAU), an investigational nucleoside analogue for chronic hepatitis B. *N Engl J Med* 1995;333(17):1099–1105.
  23. Grant J, Özkan A, Oh C, et al. Simulating drug concentrations in PDMS microfluidic organ chips. *Lab Chip* 2021;21(18):3509–3519.

---

Received December 27, 2023. Accepted August 6, 2024.

**Correspondence:**

Address correspondence to: Jonathan Z. Sexton, PhD, University of Michigan Medical School, 1150 W. Medical Center Dr, MSII Rm 4742H, Ann Arbor, Michigan 48109. e-mail: [jzsexton@umich.edu](mailto:jzsexton@umich.edu).

**Authors' Contributions:**

Conceptualization: Sophia R. Meyer, Charles J. Zhang, Jonathan Z. Sexton, Sanghee Yoo. Methodology: Sophia R. Meyer, Charles J. Zhang, Sanghee Yoo, Kyusuk Baek, Amber L. Jolly, Jiho Kim. Investigation: Sophia R. Meyer, Charles J. Zhang, Megan C. Procaro, Sumin Kim, Jiho Kim, Max A. Garcia. Data Curation: Sophia R. Meyer, Charles J. Zhang, Max A. Garcia, Roland D. Kersten. Resources: Jonathan Z. Sexton, Robert J. Fontana, Kyusuk Baek, Roland D. Kersten. Writing: Sophia R. Meyer, Charles J. Zhang, Jonathan Z. Sexton, Robert J. Fontana, Amber L. Jolly.

**Conflicts of Interest:**

These authors disclose the following: Sanghee Yoo, Amber L. Jolly, Sumin Kim, Jiho Kim, and Kyusuk Baek are affiliated with Qureator Inc, which produces the Curiochip used in this study. Robert J. Fontana has research supported by Takeda Pharmaceutical Company and Kezar Life Sciences and is a consultant for Moderna. Jonathan Z. Sexton has research support from Bristol Myers Squibb and is a consultant for Ono Pharmaceutical Co and Servier. The remaining authors disclose no conflicts.

**Funding:**

This work was supported by the National Institute of General Medical Sciences R01 award R01GM152417.

**Ethical Statement:**

This study was approved by the University of Michigan Human Pluripotent Stem Cell Research Oversight Committee (HPSCRO Record #1134).

**Data Transparency Statement:**

Images, data, and analytic methods can be made available upon a request to the corresponding author.

**Reporting Guidelines:**

ARRIVE.